Indian Geotechnical Journal, 37(4), 2007, 301-320

Effect of Stress Paths on Shear Behaviour of Clays under Lubricated End Boundary Conditions

Ajanta Sachan*

Introduction

In the past four decades, the conventional triaxial test has become the laboratory test that is most commonly used to investigate the shear strength behaviour of soil in geotechnical engineering (Bjerrum and Simons, 1960; Lowe and Johnson, 1960; Wu et al., 1962; Blight, 1963; Janbu, 1963; Lee and Seed, 1967; Balasubramaniam and Waheed, 1977; Balasubramaniam and Chaudhry, 1978; Saeedy and Mollah, 1988; Kitamura and Haruyama, 1988). A major drawback of the conventional triaxial system is the non-uniformity of stress and deformation state along the height of a specimen during externally applied load/deformation. The main source of this non-uniformity is the shear stress in the radial direction at the frictional ends, which can cause both the barrelling effect and the concentration of dilation (volume expansion due to shear) in local zones, which in turn results in the possibility of premature development of failure state. Considerable amount of research has been done in the past to improve the conventional triaxial testing apparatus and its use. Rowe and Barden (1964) used lubricated end platens in a desire to remove the dead zones within the specimen. Triaxial testing with lubricated ends was also used by Barden and McDermott (1965), Sarsby et al. (1982) to minimize the friction at the specimen ends so that the specimen deforms uniformly over its full height and provides a marked increase in the uniformity of pore pressure distribution within the clay specimen. The above experimental studies showed that in comparison to the specimens used with frictional ends, the lubricated ends perform better with shorter specimens. Rowe and Barden (1964) suggested the use of specimens with a slenderness ratio (height/diameter ratio; H/D) of 1 for testing under lubricated end conditions because it provides a more stable geometry and much greater uniformity of stress and deformation throughout the test and allows the specimen to retain its cylindrical shape even at large strains.

Rowe and Barden (1964) performed a series of undrained compression tests on sand and clay specimens with different slenderness ratio of the specimens using frictional and lubricated end platens. Their study was mostly focused on the importance of lubricated end platens and explained the advantages of using lubricated ends for clay specimens over frictional ends. Barden and McDermott (1965) used lubricated ends and performed a series of undrained compression tests on normally consolidated boulder clay and over-

* Senior Scientist, Department of Civil Engineering, Western Lab Extension, IIT-Kanpur, Kanpur, UP 208016, India. Email: ajantas@iitk.ac.in

consolidated remoulded and weathered clay. They concentrated on the use of various types of grease to prepare lubricated ends and studied the change in effective friction angle due to the change in the lubricant type. Sarsby et al. (1982) performed a series of undrained cyclic compression tests on various artificial triaxial samples composed of silicon carbide, zirconia, dolomite, and bronze by using lubricated ends. The purpose of their research was to study the errors associated with the measured axial deformation due to the compression and distortion of the rubber/grease layer when the lubricated platens were used to load particulate media. These lubricated end testing devices used in the past were not automated and not facilitated with high resolution pore pressure transducers, cell-volume control device, and volume change measurement device. Therefore, these devices did not have the capability of providing high saturation value (B) up to 0.99 and measuring excess pore pressure with high accuracy (up to 0.5 kPa).

The current research presents a microprocessor controlled fully automated lubricated end triaxial system facilitated with advanced technological measuring devices. This study also provides a brief discussion on the role of each measuring device and presents a standard procedure for performing experiments on this advanced lubricated end triaxial system. The variation in shear strength, effective friction angle (ϕ'), cohesion (c), stress strain relationship, pore pressure evolution, and effective stress paths of normally consolidated and heavily over-consolidated specimens of cohesive soil was evaluated with respect to the different stress paths (compression, extension) under lubricated end boundary conditions.

Material Properties and Specimen Preparation

The present investigation was carried out on a commercially available Kaolinite clay obtained from Akrochem Corporation, Akron, Ohio, under the trade name "Akrochem SC-25". The specific gravity, liquid limit (Casagrande apparatus), plastic limit, and grain size distribution curves were obtained in the laboratory; and the soil used in the current research was classified as unified soil. The Kaolinite clay used in this research has a liquid limit of 62 %; plasticity index of 30 %; and specific gravity of 2.63. Grain size distribution of Kaolinite clay indicates that 92% of particles are finer than 10μm, and 62% are finer than 2μm, with an activity of 0.44.

For compression and extension triaxial tests, the solid cylindrical specimens of Kaolinite clay were produced by using a two-stage slurry consolidation technique described by Penumadu et al. (1998). Figure 1 shows the setup for specimen preparation in the laboratory. The clay slurry was prepared with 155% water content corresponding to 2.5 times its liquid limit (62%), as suggested by Sheeran and Krizek (1971) to avoid the influence of the method of placement in consolidometer. Figures 1a, b, and c respectively show the prepared clay slurry, the Teflon slurry consolidometer, and the prepared clay specimen. The slurry was consolidated under K_0 condition at a vertical effective stress of 207 kPa until the primary consolidation was completed. The maximum target consolidation pressure was applied during slurry stage of the specimen in order to minimize the effect of the consolidometer wall deformation during K_0 consolidation process of specimen preparation. Solid cylindrical clay specimens of 102 mm diameter and 102 mm height were obtained after slurry consolidation, as shown in Figure 1. The clay specimens with height to diameter

ratio of 1 (slenderness ratio =1) were used in the present study as per the recommendations of Rowe and Barden (1964).

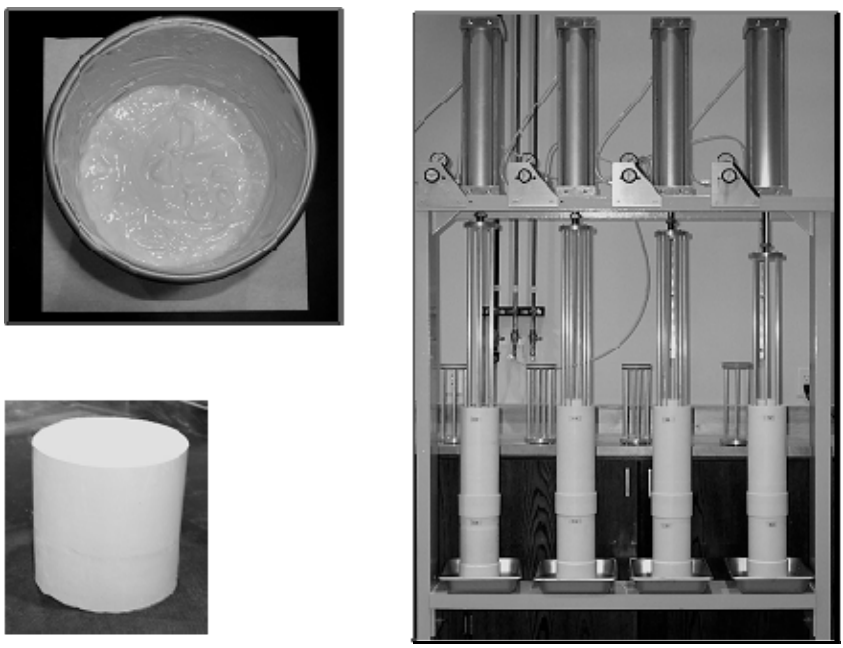

Fig. 1 Sample Preparation of Kaolinite Clay Specimen using Slurry Consolidation. (a) Prepared Clay Slurry with 155% Water Content, (b) Teflon Consolidometers with Clay Slurry at Applied Vertical Stress of 207 kPa, (c) Clay Specimen (Height=Diameter=102mm) after K_0 Consolidation

Microprocessor Controlled Automated Lubricated End Boundary Triaxial System

Preparation of Lubricated End Boundaries

A schematic diagram of the triaxial cell with lubricated ends is given in Figure 2a. Figure 2b shows a picture of polished end platen with a thin layer of silicon grease (vacuum grease) on its surface, and Figure 2c shows the location of radial drainage ports at the platen. Each platen (top and bottom) had two radial drainage ports at their outer surface, and these ports were covered by porous plastic strip that extended circumferentially to improve the drainage conditions of the testing system. In order to prepare the lubricated end platens, the steel platens were cleaned thoroughly, a thin layer of high vacuum grease was spread uniformly over each platen, and a circular piece of latex membrane (same diameter as platen and 0.3 mm thickness) was then laid on to the grease and pressed in such a way as to minimize the amount of entrapped air. It is important to note that the membrane should be chosen as thin as possible to let the specimen carry most of the load applied by the triaxial system. Then the axial stress taken by the membrane and the membrane correction should be calculated based on the thickness of the chosen membrane, and the calculated

axial stress should be deducted from the deviatoric stress. In the current research, axial stress taken by the 0.3 mm thick membrane was deducted from the deviatoric stress before calculating the corrected area of the specimen during shear deformation of soil.

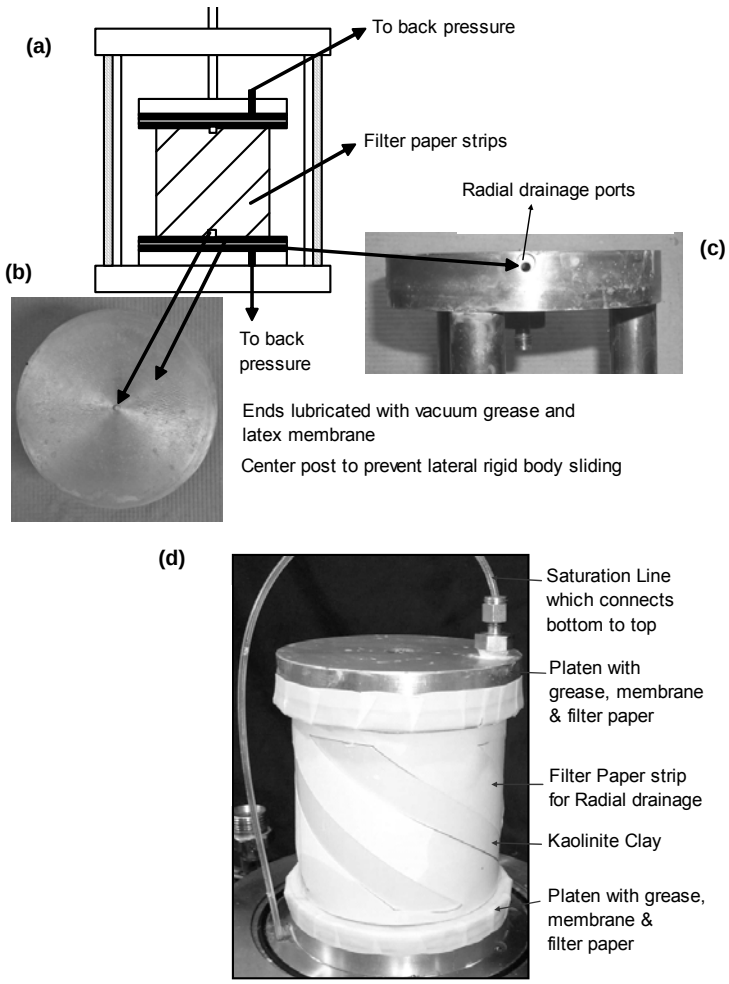

Fig. 2 Advanced Triaxial System with Lubricated End Platens. (a) Schematic Diagram of Triaxial Testing Assembly, (b) Platen with Vacuum Grease, (c) Radial Drainage Ports Located, (d) Clay Specimen (Height=Diameter=102mm) with Platens

A circular piece of filter paper, with much larger diameter than the platen was placed on top of the latex membrane in a way that the filter paper completely covered the porous plastic strip on the sides of the platens. The clay specimen was placed between the top and bottom platens and wrapped with filter paper strips facilitating the soil specimen with efficient radial drainage, as

shown in Figure 2d. Author arrived at the above reported approach to use this automated lubricated end boundary triaxial system after a large number of initial trials to optimize drainage associated with the saturated clay specimens during its consolidation and shearing stages for compression and extension stress paths.

Sensors used in Automated Lubricated End Triaxial System

This lubricated end triaxial device is fully automated and facilitated with four types of sensors, which were used to record experimental measurements at a fixed time interval. This system can record data at 10 second of time interval using VIEWDAC software program (Sachan, 2005).

1) Volume change measurement device
2) Cell volume control device
3) Three Pressure transducers
4) LVDT (Linear Variable Displacement Transducer)

Figure 3 shows the volume change measurement device, cell-volume control device, triaxial cell with Kaolinite clay specimen, and Figure 4 shows a complete picture of improved micro-processor controlled triaxial testing system with lubricated end boundary conditions.

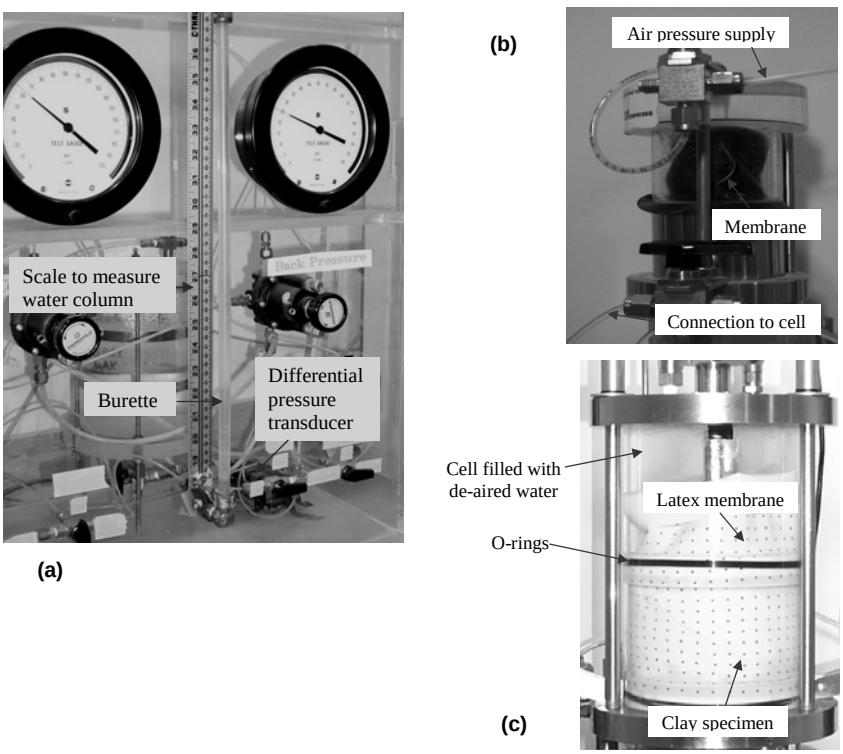

Fig. 3 Microprocessor Controlled Advanced Lubricated End Boundary Triaxial Setu (a)Volume Change Measurement Device, (b) Cell-Volume Control Device, (c) Specimen in Triaxial Cell

Figure 3a shows the volume change measurement device containing a burette and a differential pressure transducer placed on the pressure control panel. The volume of water expelled from the specimen was calculated by using the height of the water column in burette, which was measured using the differential pressure transducer connected to microprocessor. Figure 3b shows the cell-volume control device which is used in the triaxial setup to have de-aired water inside the cell. This device has a membrane of very low water-vapor transmission rate that separated the cell water from air pressure supply, and transferred the pressure without dissolving the air in the cell water. Any air dissolved in the cell water could transmit through the latex membrane in long duration tests, and significantly change the saturation level of the specimen.

Figure 3c shows a cylindrical Kaolinite clay specimen placed inside the triaxial cell filled with de-aired water attached with three pressure transducers, which are used to monitor the triaxial cell pressure, and the pore pressure values at the top and bottom of the soil specimen. The LVDT was mounted on the top plate of triaxial cell to measure the displacement, which was used to calculate the change in height of the specimen during various stages of the test. Figure 4 shows an overall configuration of the test setup including a clay specimen inside the triaxial cell attached with the pressure control panel, data acquisition system and other electronics, and an attached microprocessor that records consolidation and shear data throughout the test.

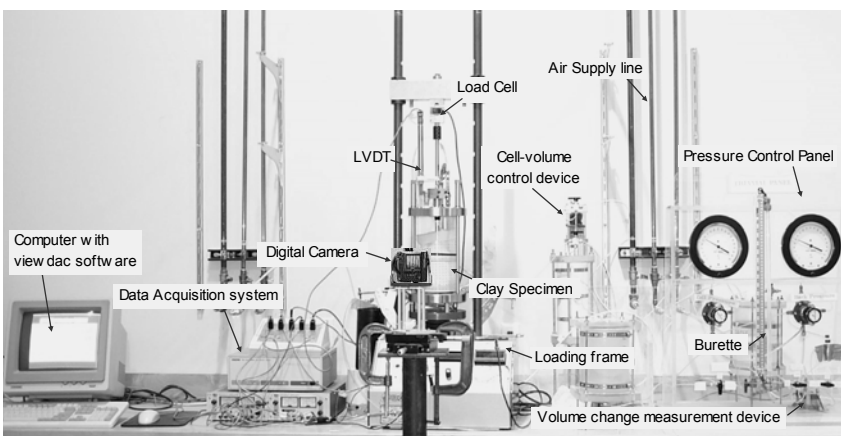

Fig. 4 A complete setup for Improved Microprocessor Controlled Triaxial System with Lubricated End Boundary Conditions

Standard Procedure

Saturation

After assembling the clay specimen in a custom-built triaxial cell as explained above, three pressure transducers were attached to the triaxial system for measuring the pore pressure at top and bottom of the specimen, and the cell pressure. The assembly followed the general procedure of ASTM: D4767-95 for consolidated undrained triaxial compression tests for cohesive soils. To saturate the specimen-boundary interfaces, the system was flushed

with CO_2 initially, and then purged with de-aired, de-ionized water. Back pressure was used to dissolve any trapped CO_2 into the solution and to ensure proper saturation level of the specimen. A back pressure of 172 kPa was applied to all the test specimens throughout the consolidation and shearing processes. In all the tests, the measured Skempton's pore pressure parameter (B) during saturation check was greater than 0.99 indicating that a high degree of saturation was achieved prior to the application of shear stress. It is important to note that very few researchers have reported the higher degree of saturation in their experimental observations. The lower value of B obtained in fine grained cohesive materials would lead to the inaccurate measurement of excess pore pressure evolution and stress-strain behaviour during the shear deformation of soil specimen. Thus, it is extremely important to achieve B value close to 0.99 before moving to next phase of triaxial testing (consolidation, shearing).

Isotropic Consolidation and Shearing

After saturation, the specimen was isotropically consolidated under the chosen effective confining pressure (207, 276, and 345 kPa). Radial drainage provided by the filter paper strips on the outer surface of the specimen reduced the necessary time for consolidation and pore pressure equalization. The volume change of the specimen was measured throughout the consolidation process. After completion of isotropic consolidation, a displacement controlled axial loading frame (Geotest, Model No. S5761) was used to apply the axial load on the specimen simulating compression and extension stress paths. In compression and extension shearing, loads were applied on isotropically consolidated clay specimen by allowing the bottom platen of triaxial loading frame to move in upward direction for compression shearing and in downward direction for extension shearing while top platen was kept fixed. In compression shearing, radial stress was acting as minor principal stress (σ_3) and axial stress as major principal stress (σ_1). However, in extension shearing, radial stress was acting as major principal stress (σ_1) and axial stress as minor principal stress (σ_3) based on the value of axial stress smaller than radial stress due to the downward movement of bottom platen.

Effect of Compression and Extension Stress Paths on Shear Behaviour of Clays under Lubricated End Boundary Conditions

Using the microprocessor controlled automated lubricated end boundary triaxial system, a series of isotropically consolidated triaxial compression and extension tests were conducted on normally consolidated (overconsolidation ratio; OCR =1) and heavily overconsolidated (OCR =10) Kaolinite clay specimens (Height=Diameter=102 mm) at three pre-consolidation pressures (p_o' = 207, 276, and 345 kPa), as shown in Table 1. All the clay specimens were sheared under undrained conditions at the strain rate of 0.05% per min ensuring excess pore pressure equilibration during shear. A good repeatability of experimental data was achieved during this testing program. Figure 5 shows a typical example of the repeatability using the stress-strain curves and effective stress paths (q Vs p' curve) for repeated triaxial compression tests on NC and HOC clay with pre-consolidation pressure (p_o') of 276 kPa. The values of q and p' were calculated using Equation 1 and 2 respectively.

$$q = (\sigma_1' - \sigma_3') \quad (1)$$

$$p' = (\sigma_1' + \sigma_2' + \sigma_3')/3 \quad (2)$$

Table 1: List of Triaxial Experiments Performed on Kaolin Clay Specimens with the use of Lubricated End Platens

No.	Type	Loading	OCR	p_0' (kPa)	(σ_c') (kPa)
1.	CIU	Compression	1	207	207
2.	CIU	Compression	1	276	276
3.	CIU	Compression	1	345	345
4.	CIU	Compression	10	207	21
5.	CIU	Compression	10	276	28
6.	CIU	Compression	10	345	35
7.	CIU	Extension	1	207	207
8.	CIU	Extension	1	276	276
9.	CIU	Extension	1	345	345
10.	CIU	Extension	10	207	21
11.	CIU	Extension	10	276	28
12.	CIU	Extension	10	345	35

No: - Test Number, Type - Type of Triaxial Test
Load - Loading Conditions, OCR - OCR value
p_0' - Effective pre-consolidation pressure (kPa)
σ_c' - Effective confining pressure during shear deformation (kPa)

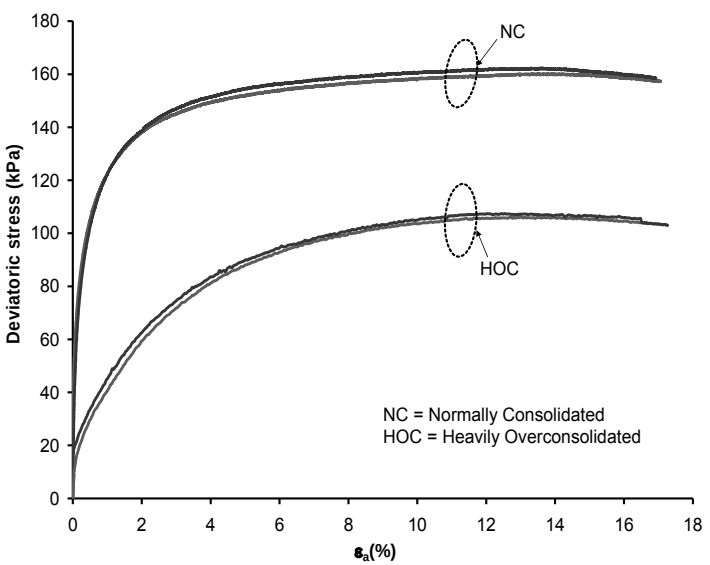

Fig. 5a Compression Test Data of Kaolinite Clay (p'_o =276 kPa) for Showing Repeatability. (a) Stress-Strain Curves, (b) Effective Stress Paths

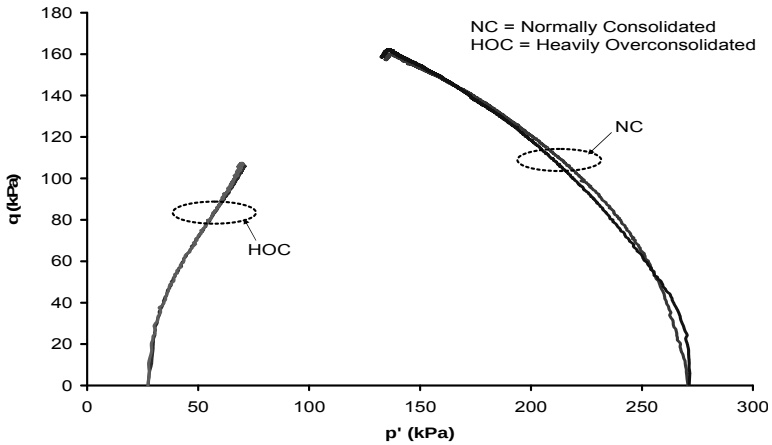

Fig. 5b Compression Test Data of Kaolinite Clay (p'_o =276 kPa) for Showing Repeatability. (a) Stress-Strain Curves, (b) Effective Stress Paths

Normalization Criteria

There are two ways of normalizing the stress paths that many researchers have used in previous studies for normally and overconsolidated clays. In one method, the stresses are normalized by the pre-shear effective confining pressure (σ_c') and in the other method by the effective pre-consolidation pressure before shearing (p_o'). The effective stress paths normalized by the σ_c' for triaxial compression tests on NC and HOC Kaolinite clay specimens are presented in Figure 6.

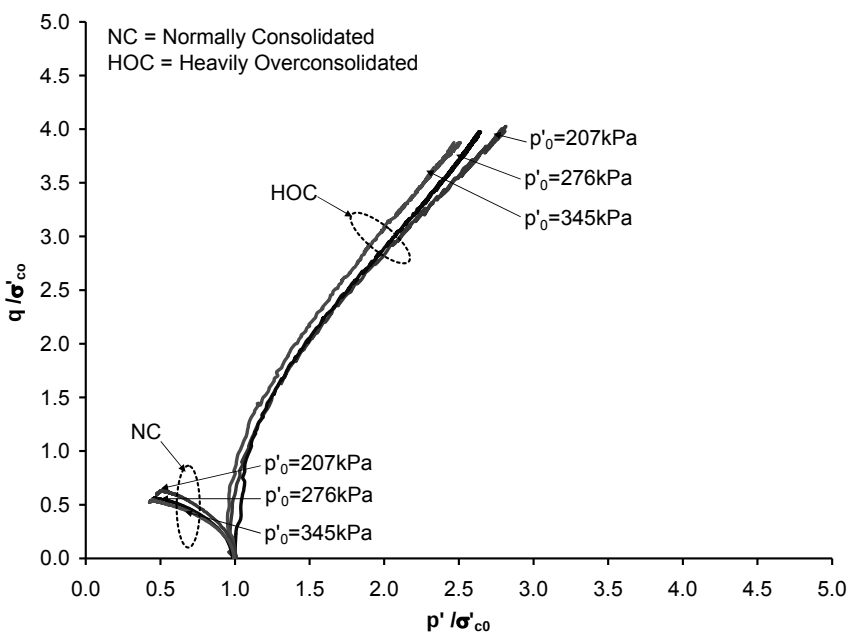

Fig. 6 Normalized Effective Stress Paths (Normalization with σ'_c) for Compression Tests on NC and HOC Specimens

This figure shows that the normalization method using σ_c' resulted in a large variation between the normalized values of deviator stress corresponding to NC and HOC clay. These normalized effective stress paths indicate that the shear stiffness and strength of the HOC clay would be much higher in comparison to NC clay at the same effective confining pressure. This could be attributed to the fact that the HOC clay would have much lower void ratio than the NC clay at the same value of confining pressure. In order to incorporate the influence of void ratio (e), the normalization method using p_o' was used for normalizing the stress path, shear behavior, and pore pressure response of clay. The normalization method using p_o' was a common technique used in most of the volumetric hardening constitutive models, such as the critical state model (Schofield and Wroth, 1968). It is important to note that the values of σ_c' used for triaxial tests on NC clay were 207, 276, and 345 kPa, and for the tests on HOC clay, they were 21, 28, and 35 kPa. Therefore, the three values of pre-consolidation pressure used for the triaxial tests on HOC clay were the same as for the tests on NC clay (p_o' = 207, 276, 345 kPa). Thus, it was reasonable to normalize the stress-strain excess pore pressure evolution, and effective stress path by using p_o' instead of σ_c'.

Pore-pressure Evolution

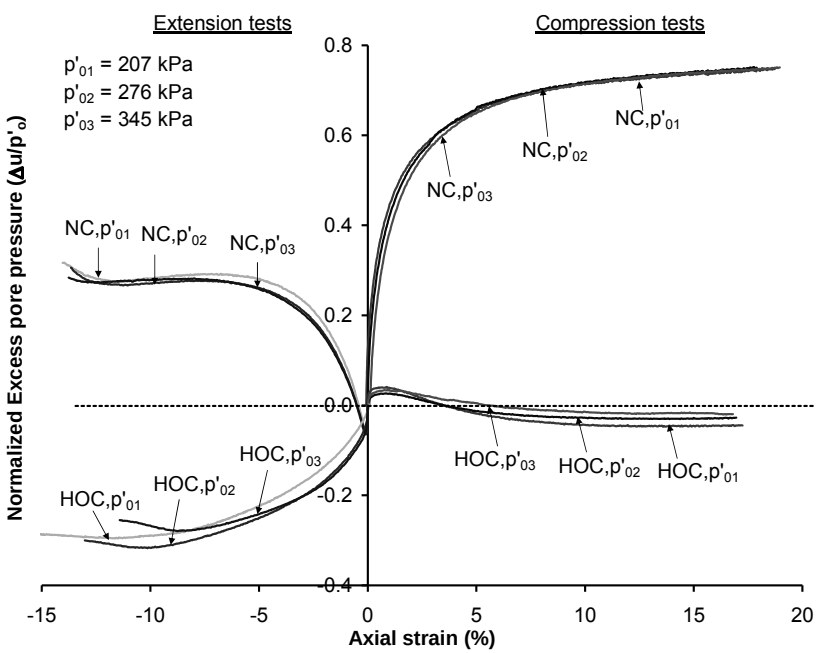

Fig. 7 Normalized Excess Pore Pressure Behavior for Compression and Extension Stress Paths

Figure 7 shows the excess pore pressure evolution normalized by p_o' for the triaxial compression and extension tests on NC and HOC specimens. The normalized excess pore pressure evolution for NC clay was observed to be

much stronger for compression shearing than that for extension shearing at a given confining stress. However, normalized excess pore pressure evolution for HOC clay exhibited significantly lower values for compression shearing than that for extension shearing. The reason could be that the extension shearing disturbed the closely packed arrangement of the Kaolinite clay particles and particle groups by pulling them away from each other; however, compression shearing helped them to move towards each other; and this generated or enhanced the dilative nature of Kaolinite clay. NC specimens are generally believed to be contractive in nature, but extension shearing of NC specimens of Kaolinite clay exhibited dilative response at early stage of shearing under lubricated end boundary conditions. It has been previously reported (Rowe and Barden, 1964; Barden and McDermott, 1965) that the effect of boundary conditions on soil specimen is significantly reduced by using lubricated end platens as compared to frictional end platens (conventional triaxial system); thus dilative behavior of Kaolinite clay specimen during extension shearing is not due to its end conditions, but due to its volumetric characteristics. HOC specimens are believed to be dilative in nature, and extension shearing enhanced their dilative nature (Figure 7).

The compression tests on HOC clay exhibited a trend of slightly increasing normalized excess pore pressure evolution (negative values) with the decreasing p_o'; however, no pattern could be detected for the extension tests on HOC clay. NC specimens also exhibited no pattern for its normalized excess pore pressure response with respect to p_o' for both the stress paths. For all the practical purposes, the excess pore pressure evolution could reasonably be assumed as a linear function of p_o' (since variation was insignificant when u was normalized with p_o') for all triaxial tests performed in the current research.

Stress-Strain Relationship

Figure 8 shows the relationship between the deviator stress normalized by p_o' and axial strain during undrained shearing. This figure shows the data for compression and extension tests on both NC and HOC Kaolinite clay specimens. The stress-strain relationships for compression tests did not indicate well-defined peaks as those were observed in extension tests. Perhaps, this behavior could be attributed to the inherent instability that develops in the deforming specimen under triaxial extension loading conditions at high strain levels. During extension shearing, the specimen tends to have a smaller cross-sectional area at the middle of the clay specimen compared to the area at top and bottom of the specimen. This makes the clay specimen weak and unstable when subjected to a large amount of shear deformation, and leads to strain localization within the soil element. During compression testing, the cross-sectional area of the specimen increases; and therefore, a tendency for such instability does not exist.

However, the specimen under compression loading may still undergo other modes of strain localization close to peak shear stress location due to material imperfections. It is important to note that the instability due to application of axial loading method and conditions was significantly reduced with the use of lubricated end platens in the present research. Figure 9 shows the pictures of sheared Kaolinite clay specimens subjected to extension and compression shearing during this study. The cross-sectional area of section 2-2 was found to be significantly smaller than the area of section 1-1 in extension

tests; however, the area of both the cross-sectional area at top and bottom of specimen during compression test was observed to be fairly similar.

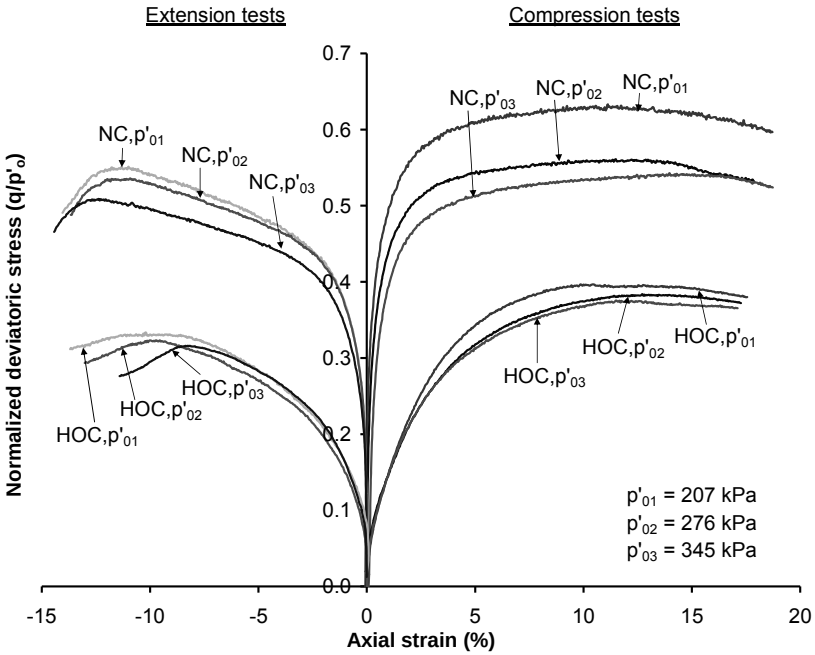

Fig. 8 Normalized Stress-Strain Response for Compression and Extension Stress Paths

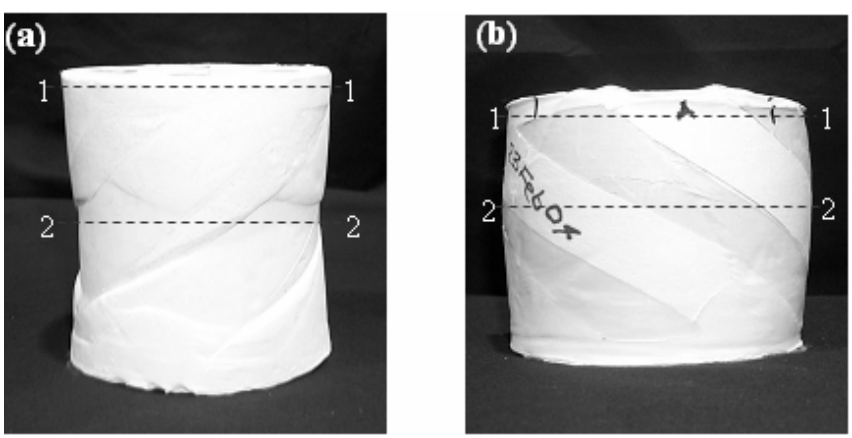

Fig. 9 Kaolinite Clay Specimens after Shearing at 18% Strain Levels using Lubricated End Triaxial Setup. (a) Extension Test, (b) Compression Test

In all the compression and extension triaxial tests, the normalized deviator stress was decreased when p_o' increased. The change in normalized deviator stress due to the variation in p_o' was found to be much stronger for NC clay than that for HOC clay, which can be rationalized by considering the absolute difference in the values of σ_c' for NC and HOC specimens of Kaolinite clay. The applied σ_c' values in the current study were 207, 276, and 345 kPa for NC clay and 21, 28, and 35 kPa for HOC clay. Therefore the corresponding variation in effective cell pressure (σ_c') difference for a given p_o' was found to be 69 kPa for NC and 7 kPa for HOC clay. The small variation of σ_c' values for HOC clay contributed to a correspondingly small variation in deviator stress. Therefore, the confining pressure showed a stronger influence on the shear deformation behaviour of NC clay than HOC clay.

Effective Stress Path

Figure 10 shows the effective stress paths (compression or extension test) of NC and HOC clay, and the stress states are normalized by p_o'. The normalized effective stress paths for triaxial compression tests on NC clay showed a marked influence of the p_o' values; whereas, the effective stress paths for extension tests for NC clay exhibited little variation with respect to p_o'. The pattern of effective stress path during undrained shearing could depend on both the shear stiffness and the volumetric tendency of the soil.

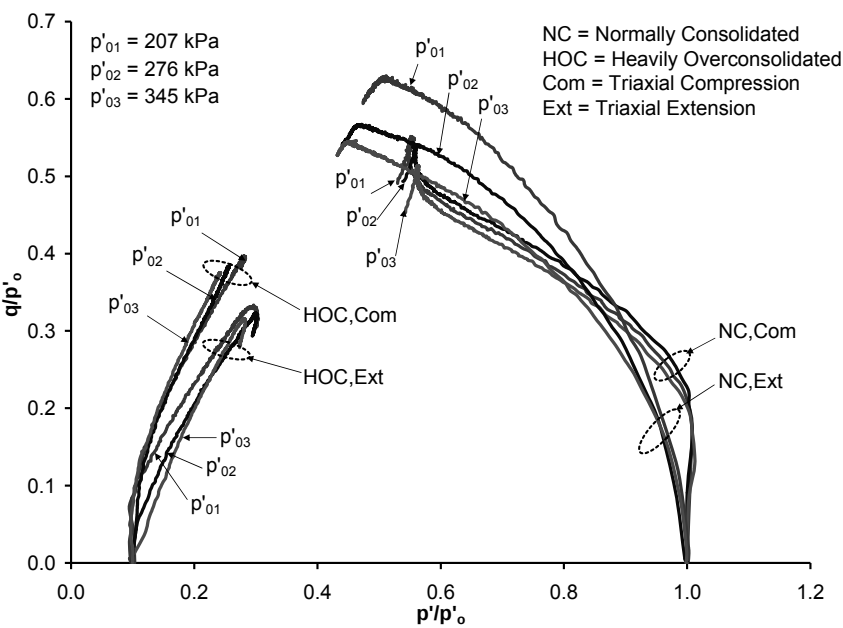

Fig. 10 Normalized Effective Stress Paths for Undrained Compression and Extension Triaxial Tests under Lubricated End Boundary Conditions

The pore pressure evolution was observed to be linearly dependent on p_o' (Figure 7). Therefore, the observed variation in the normalized effective stress paths for NC clay was due to the non-linear dependency of shear

stiffness on p_o', as was shown by the shear stress-strain relationships in Figure 8. The normalized effective stress paths of NC clay show a decreasing trend as p_o' increased for both compression and extension loading conditions, and therefore, the effective stress paths were not linearly dependent on p_o'. The normalized effective stress paths for HOC clay did not show significant variation with respect to the change in p_o' values due to the small difference of effective cell pressure ($\Delta\sigma_c$'=7 kPa) applied during HOC stress state, as was explained earlier. For NC clay, effective stress paths tend to shift towards the origin at higher strain levels; however, effective stress paths for HOC clay tend to go away from the origin. This behaviour could also be interpreted as the normally consolidated clay being contractive and overconsolidated clay being dilative in nature during shearing. This behaviour was observed to be the same for both compression and extension loading conditions.

Shear Strength Parameters

Table 2 presents a summary of the shear strength parameters obtained from various triaxial undrained tests performed on Kaolinite clay specimens with different stress histories for two different stress paths; compression and extension.

Hvorslev (1960) reported that "the values of c_e' and ϕ_e' are not the actual cohesion or angle of internal friction but merely mathematical components". Using Hvorslev's approach the values of apparent cohesion and angle of internal friction were calculated for the experimental data from the current study and the values are listed in Table 2a. Undrained shear strength for extension shearing was observed to be significantly smaller than that for compression shearing due to soil's dilative or less contractive nature during extension testing under lubricated boundary conditions.

The effective friction angle for extension testing was observed to be significantly higher than that for compression testing. For NC and HOC clay, the effective friction angle (ϕ_e') was found to decrease with an increase in the p_o' for both compression and extension tests. HOC clay also showed a marked increase in the apparent cohesion (c_e') of Kaolinite clay with the rise in p_o' value, and this indicates that the effective cohesion is a function of p_o', as reported by Hvorslev (1960).

Since the clay specimens used in the current study were slurry consolidated in the laboratory and did not experience aging before triaxial testing; therefore, the true cohesion for this clay could be assumed to be zero. Therefore, the tests performed at different confining pressure at the same overconsolidation level can be analyzed using no cohesion (c'=0) for determining the Mohr-Coulomb's failure parameters. Based on this approach, the values of ϕ' were calculated at different confining pressures for HOC clay, as shown in Table 2b. Within the range of effective confining pressure used in this study, the effective friction angle (ϕ') for overconsolidated specimens showed a marked increase with increasing pre-consolidation pressure (p_o') values for both compression and extension stress paths. It is important to note that effective friction angle for compression shearing was observed to be significantly smaller than that for extension shearing; and this is true for both the analysis; i) using Hvorslev approach, ii) considering no aging effect.

Table 2: Shear Strength Properties of Kaolinite Clay during Undrained Shearing.
(a) Using Hvorslev's Approach, (b) No Aging effect (c'= 0 for HOC)

(a)

p_0' (kPa)	σ_c' (kPa)	q (kPa)	S_u (kPa)	ε_a (%)	η_f (q/p')	σ_1'/σ_3'	c_e' (kPa)	ϕ_e' (deg.)	A_f	Λ_0
Compression tests performed on normally consolidated (OCR 1) clay specimens										
207	207	127.1	63.6	11.1	1.27	3.21	0.0	31.7	1.08	-
276	276	154.5	77.3	11.5	1.20	3.00	0.0	30.1	1.24	-
345	345	186.5	93.3	14.0	1.18	2.94	0.0	29.5	1.29	-
Compression tests performed on heavily overconsolidated (OCR 10) clay specimens										
207	21	82.1	41.1	10.0	1.42	3.69	9.5	27.5	-0.11	0.81
276	28	106.3	53.2	12.7	1.49	3.99	22.0	21.8	-0.07	0.84
345	35	129.6	64.8	11.5	1.56	4.82	32.0	19.5	-0.05	0.84
Extension tests performed on normally consolidated (OCR 1) clay specimens										
207	207	114.5	57.3	11.0	1.01	4.10	0.0	37.4	1.54	-
276	276	147.2	73.6	11.0	0.97	3.72	0.0	35.2	1.55	-
345	345	176.6	88.3	12.7	0.91	3.33	0.0	32.6	1.57	-
Extension tests performed on heavily overconsolidated (OCR 10) clay specimens										
207	21	68.0	34.0	10.6	1.11	4.40	10.0	31.4	0.01	0.75
276	28	89.5	44.8	10.0	1.12	4.82	13.5	29.0	0.01	0.78
345	35	108.9	54.5	8.5	1.13	5.55	25.6	23.4	0.08	0.79

(b)

Type of testing	p_0' (kPa)	q (Kpa)	ϕ' (deg.)
Compression tests on HOC clay	207	82.1	35.0
	276	106.3	37.0
	345	129.6	41.0
Extension tests on HOC clay	207	68.0	39.0
	276	89.5	41.0
	345	108.9	44.0

S_u = Undrained shear strength; ε_a =Axial strain at failure; η_f = Shear stress ratio (q/p'); σ_1'/σ_3' =Effective stress ratio; ϕ_e'= Apparent cohesion.
All the test data represents the values at failure.

The effective friction angle of NC specimens of Kaolinite clay (LL = 62%, PI = 30%, activity = 0.44) from this study was observed to be in the range of 29.5° to 31.7° during compression shearing at various effective confining pressure levels (207, 276, and 345 kPa). Seed and Mitchell (1960) reported 24° of ϕ' value for Kaolinite clay (LL = 47%, PI = 16%) by performing compression tests on NC specimens using frictional ends at 98 kPa of confining pressure. Broms and Ratnam (1963) performed frictional end triaxial compression tests on NC specimens (slenderness ratio=2) of Kaolinite clay (LL = 48%, PI = 15%, activity = 0.38) at the effective confining pressure of 637 kPa, and obtained the ϕ' value of 24.5° . Sridharan et al. (1971) observed ϕ' = 25.5° for Kaolinite clay (LL = 49%, PI = 20%) by performing compression tests on NC clay specimens (slenderness ratio=2) at 207 kPa of confining pressure using lubricated ends. The current research showed the largest value of ϕ' for Kaolinite clay using microprocessor controlled automated lubricated end boundary triaxial system in comparison to the reported values in previous studies using conventional triaxial system or old lubricated end triaxial system. Other reasons could be that the Kaolinite clay used in the current study has comparatively higher liquid limit and plasticity index than the clay used previously, and the use of clay specimens with slenderness ratio 1 possibly providing the higher value of effective friction angle.

The shear stress ratio (η_f), which is the ratio of deviator stress q and mean effective stress p' at failure (Equation 1 and 2), was calculated for various triaxial tests. The η_f value decreased for NC clay and increased for HOC clay as the p_o' increased for both the compression and the extension stress paths. Having a relationship with shear stress ratio (η_f), the effective stress ratio (σ_1'/σ_3') at failure showed a similar pattern for NC and HOC clay, as listed in Table 1. Skempton and Bishop (1954) pore pressure parameters (A_f) is used in practice to estimate the pore pressure response of soil at failure conditions. A_f can be calculated by using Equation 3. The parameter B was assumed to be 1 for saturated clay specimens in this research. Pore pressure parameter (A_f) was found to be significantly higher for extension tests than for compression tests. Pore pressure parameter (A_f) was observed to be fairly stable with the variation in p_o' for all cases; triaxial compression and extension tests on Kaolinite clay with OCR values 1 and 10. The average value of A_f at three different confining pressures was obtained to be 1.25 for compression tests and 1.55 for extension tests indicating the significant impact of stress paths.

$$A_f = \frac{\Delta u_f - B.\Delta\sigma_{3f}}{\Delta\sigma_{1f} - \Delta\sigma_{3f}} \tag{3}$$

Mayne (1979) introduced an empirical relationship (Eq. 4) for normalizing the undrained shear strength of over-consolidated (OC) clay and normally consolidated (NC) clay.

$$OCR^{\Lambda_0} = \frac{(s_u / p_o')_{OC}}{(s_u / p_o')_{NC}} \tag{4}$$

The parameter Λ_0 was reported to be constant for a particular soil in the study performed by Mayne (1979). As shown in Table 2, the value of Λ_0 did

not change significantly for the variation of p_o' (69 kPa) at certain type of anisotropic loading conditions. The approximate value of Λ_0 for compression and extension testing were determined to be 0.82 and 0.77 respectively.

Conclusions

A microprocessor controlled automated lubricated end boundary triaxial system facilitated with high resolution pore pressure transducers, cell-volume control device, and volume change measurement device was used in this research with the facility of providing high saturation value (B-value) up to 0.99 and pore pressure & cell pressure measurements with high accuracy (0.5 kPa).

Using this automated lubricated end triaxial system, a series of undrained compression and extension tests were performed on NC and HOC specimens of Kaolinite clay at different confining stress levels. A comparative study was also performed for evaluating the impact of stress paths on the shear behavior of soil at different stress states (NC, HOC) considering the values of shear strength, effective friction angle, cohesion, stress ratio, and pore pressure parameter at failure for the tests performed at three different confining pressure values. The presented data could be valuable for the purpose of mathematical modeling such as constitutive model, artificial neural network model.

The normalized excess pore pressure evolution for NC clay was observed to be much stronger for compression shearing than that for extension shearing at given confining stress level. However, pore pressure evolution for HOC clay exhibited significantly lower values for compression shearing in comparison to extension shearing.

For all the compression and extension tests, the excess pore pressure response was observed to be a linear function of pre-consolidation pressures (p_o'). The stress-strain relationships for compression tests did not indicate well-defined peaks as those were observed in extension tests due to the instability generated within the specimen induced by extension shearing. The normalized stress-strain relationships and effective stress paths for NC clay were observed to have a decreasing trend with increasing p_o' values for both compression and extension stress paths.

The HOC clay showed a similar trend for normalized stress-strain relationships and effective stress paths as observed for NC clay. Undrained shear strength for extension stress path was observed to be significantly smaller than that for compression stress path. The effective friction angle (ϕ_e') was observed to be significantly higher for extension shearing than for compression shearing for both NC and HOC clay.

HOC clay exhibited an increasing trend of apparent cohesion (c_e') and a decreasing trend of effective friction angle (ϕ_e') as p_o' increased (using Hvorslev's approach) for both compression and extension stress paths.

Acknowledgements

The author is highly thankful to Dr. Dayakar Penumadu, Professor at University of Tennessee, Knoxville, USA for his help, guidance, and encouragement during this study. Financial Support from National Science

Foundation (NSF) through grants CMS-9872618 and CMS-0296111 is gratefully acknowledged. Any opinions, findings, and conclusions or recommendations expressed in this material are those of author and do not necessarily reflect the views of NSF.

Notations

B = Saturation Value

c_e' = Apparent Cohesion (Hvorslev's approach)

ϕ'_e = Effective friction angle (Hvorslev's approach)

HOC = Heavily Overconsolidated

η_f = Shear Stress Ratio (q/p')

NC = Normally Consolidated

OCR = Overconsolidation Ratio

p'_o = Pre-consolidation pressure

q , p' = Deviator stress and mean effective stress in invariant form

S_u = Undrained shear Strength

σ_1' = Major principal stress

σ_3' = Minor principal stress ($\sigma_3' = \sigma_2'$ in the current study)

σ_1'/σ_3' = Effective stress ratio

$\Delta\sigma_{1f}$ = Change in Major principal stress at failure conditions

$\Delta\sigma_{3f}$ = Change in Minor principal stress at failure conditions

Δu_f = Excess pore pressure at failure conditions

ϕ' = Angle of internal friction

Λ_0 = Mayne's pore pressure parameter (mentioned in Mayne 1979)

References

ASTM (1995), "Standard test method for consolidated undrained triaxial compression test for cohesive soils," D4767-95*,* West Conshohocken, PA.

Balasubramanium, A.S. and Waheed, U. (1977), "Deformation characteristics of weathered Bangkok clay in triaxial extension," *Geotechnique*, Vol. 27, No. 1, pp. 75-92.

Balasubramanium, A.S. and Chaudhry, A.R. (1978), "Deformation and strength characteristics of soft Bangkok Clay," *Journal of the Geotechnical Engineering Division*, ASCE, Vol. 104, No.GT9, pp. 1153-1167.

Barden, L. and Mcdermott, R.J.W. (1965), "The use of Free Ends in Triaxial Testing of Clays," *Journal of the Soil Mechanics and Foundation Division*, ASCE, Vol. 91, No. SM6, pp. 1-23.

Bjerrum, L. and Simons, N. (1960), "Comparison of Shear strength characteristics of Normally-Consolidated Clays," *Shear Strength of Cohesive Soils*, ASCE, pp. 711-726.

Blight, G.E. (1963), "The Effect of nonuniform pore pressures on Laboratory measurements of the shear strength of soils," *Symposium on Laboratory Shear Testing of soil*, ASTM S.T.P. 361, pp. 173-184.

Broms, B. and Ratnam, M. (1963), "Shear Strength of an anisotropically-consolidated clay," *Journal of the Soil Mechanics and Foundations Engineering*, Vol. 89, pp. 1-26.

Hvorslev, M. J. (1960), "Physical Components of the Shear Strength of Saturated Clays," *ASCE Research Conf. on Shear Strength of Cohesive Soils*, University of Colorado, Boulder, Colorado, pp. 69-273.

Janbu, N. (1963), "Soil compressibility as determined by oedometer and triaxial tests," *European conference on soil mechanics and Foundation Engineering*, Germany, Vol. 1, pp. 19-25.

Kitamura, R. and Haruyama, M. (1988), "Compression and shear deformation of soil under wide-ranging confining pressure," *Advanced triaxial testing of soil under wide-ranging confining pressure*, ASTM STP 977, pp. 501-511.

Lee, K.L. and Seed, H.B. (1967), "Drained strength characteristics of sands," *Journal of the Soil Mechanics and Foundation Division*, ASCE, Vol. 93, No. SM6, pp. 117-141.

Lowe, J. and Johnson, T.C. (1960), "Use of Back Pressure to increase degree of saturation of Triaxial Test Specimen," *Shear Strength of Cohesive Soils*, ASCE, pp. 819-836.

Mayne, P.W. (1979), "Discussion of 'Normalized deformation parameters for Kaolin' by H.G. Poulos," *Geotechnical Testing Journal,* ASTM, Vol. 2, No. 2, pp. 118-121.

Penumadu, D., Skandarajah, A. and Chameau, J.L. (1998), "Strain-rate effects in pressuremeter testing using a cuboidal shear device: Experiments and Modeling," *Canadian Geotechnical Journal*, Vol. 35, pp. 27-42.

Rowe, P.W. and Barden, L. (1964), "Importance of Free Ends in Triaxial Testing," *Journal of the Soil Mechanics and Foundation Division,* ASCE, Vol. 90, No. SM1, pp. 1-27.

Sachan, A. (2005), "Identification of the Microfabric of Kaolin clay and its impact on the shear strength behavior", *PhD. Thesis, University of Tennessee, Knoxville*,TN, USA.

Saeedy, H.S. and Mollah, M.A. (1988), "Application of Multistage Triaxial test of Kuwaiti soils," *Advanced Triaxial Testing of Soil and Rock*, ASTM STP 977, pp. 363-375.

Sarsby, R.W., Kalteziotis, N. and Essam, H.H. (1982), "Compression of "Free-ends" during triaxial testing," *Journal of the Geotechnical Engineering Division,* ASCE, Vol. 108, No.GT1, pp. 83-107.

Schofield, A.N. and Wroth, C.P. (1968), "Critical state soil mechanics," *London, McGraw-Hill.*

Seed, H.B. and Mitchell, J.K. (1960), “The strength of Compacted Cohesive Soils,” *Shear Strength of Cohesive Soils*, ASCE, pp. 877-964.

Sheeran, D.E. and Krizek, R.J. (1971), “Preparation of Homogenous soil samples by slurry consolidation,” *Journal of Materials,* Vol. 6, No. 2, pp. 356-373.

Skempton, A.W. and Bishop, A.W. (1954), “Soils Chapter 10 of Building Materials,” *North Holland Publication Co.,* pp. 471-482.

Sridharan, A., Rao, S. and Rao, G. (1971), “Shear strength characteristics of saturated Montmorillonite and Kaolin clays,” *Soils and Foundations*, Vol. 11, pp. 1-22.

Wu, T., Douglas, A. and Goughnour, R. (1962), “Friction and Cohesion of saturated clays,” *Journal of the Soil Mechanics and Foundation Division*, ASCE, Vol. 90, No. SM3, pp. 1-32.